

**Modulating the periods and electronic properties of striped moiré  
superstructures for monolayer WSe<sub>2</sub> on Au(100) by varied  
interface coupling**

Zehui Zhang,<sup>a</sup> Jingyi Hu,<sup>b</sup> Pengfei Yang,<sup>b</sup> Shuangyuan Pan,<sup>a</sup> Wenzhi Quan,<sup>b</sup> Ning Li,<sup>a</sup> Lijie Zhu,<sup>a</sup> and Yanfeng Zhang<sup>\*a</sup>

<sup>a</sup> School of Materials Science and Engineering, Peking University, Beijing 100871, People's Republic of China

<sup>b</sup> Academy for Advanced Interdisciplinary Studies, Peking University, Beijing 100871, People's Republic of China

\*Address correspondence: [yanfengzhang@pku.edu.cn](mailto:yanfengzhang@pku.edu.cn)

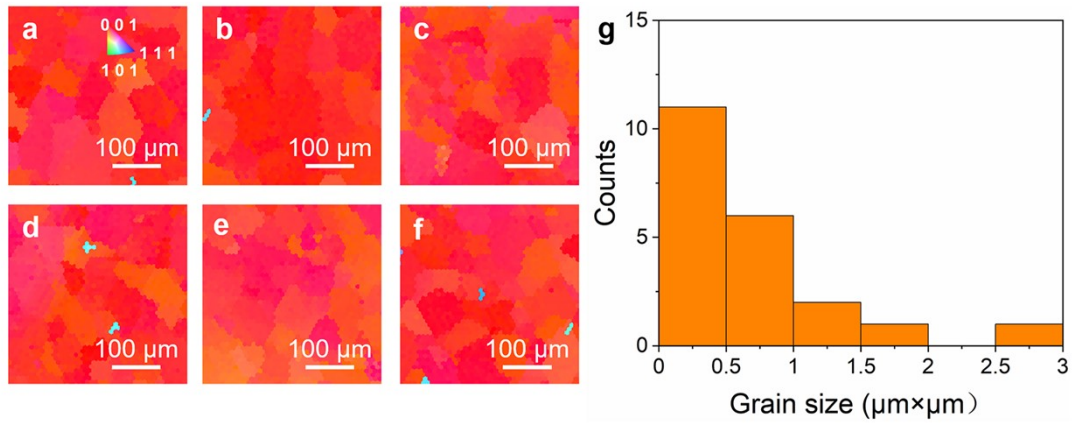


**Figure S1.** Typical grain size statistics of the Au(100) facet. (a-f) EBSD maps from six local regions, respectively. (g) Statistical histogram of the grain sizes of the Au(100) facet.

According to the statistical results, grain sizes of the Au(100) facet are mainly distributed within 0-1  $\mu\text{m}^2$ . Treatment of Au foils: Polycrystalline gold foils were first ultrasonically cleaned, and then loaded into the CDW chamber for a long standard annealing treatment time ( $\sim 950$  °C for 5 h in atmosphere).

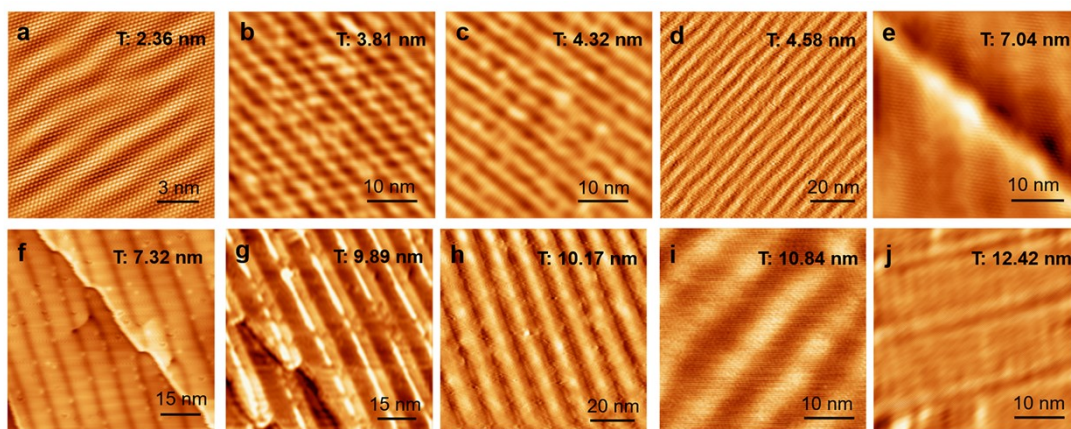


**Figure S2.** STM characterizations of striped moiré superstructure patterns for monolayer WSe<sub>2</sub> on Au(100) after annealing process at ~340 °C. “T” represents the periodicities or the inter-stripe distances for striped moiré superstructures.

After ~340 °C annealing process, the typical morphology of the striped moiré superstructure patterns for monolayer WSe<sub>2</sub> on Au(100) was obtained, as shown in Figure S2. The periodicities of striped patterns fall in a range of 0-15 nm, indicating nearly random orientations of monolayer WSe<sub>2</sub> domains on the Au(100) facet.

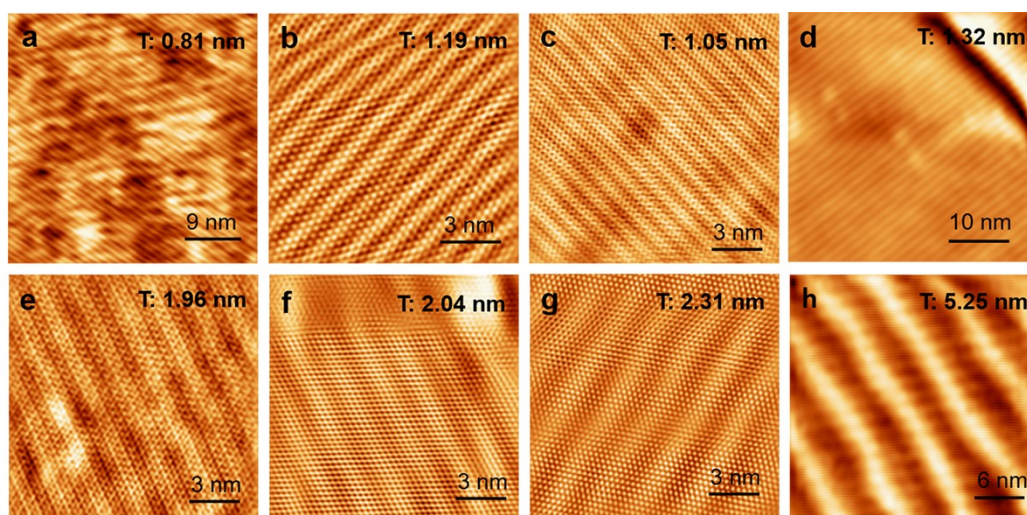


**Figure S3.** STM characterizations of striped moiré superstructures for monolayer WSe<sub>2</sub> on Au(100) after sample annealing process at ~420 °C for 4h.

After high-temperature annealing process at ~420 °C for 4h, the morphology of the striped moiré superstructure patterns for monolayer WSe<sub>2</sub> on Au(100) was achieved, as shown in Figure S3. The periodicities of the striped moiré superstructures fall in a narrow range.

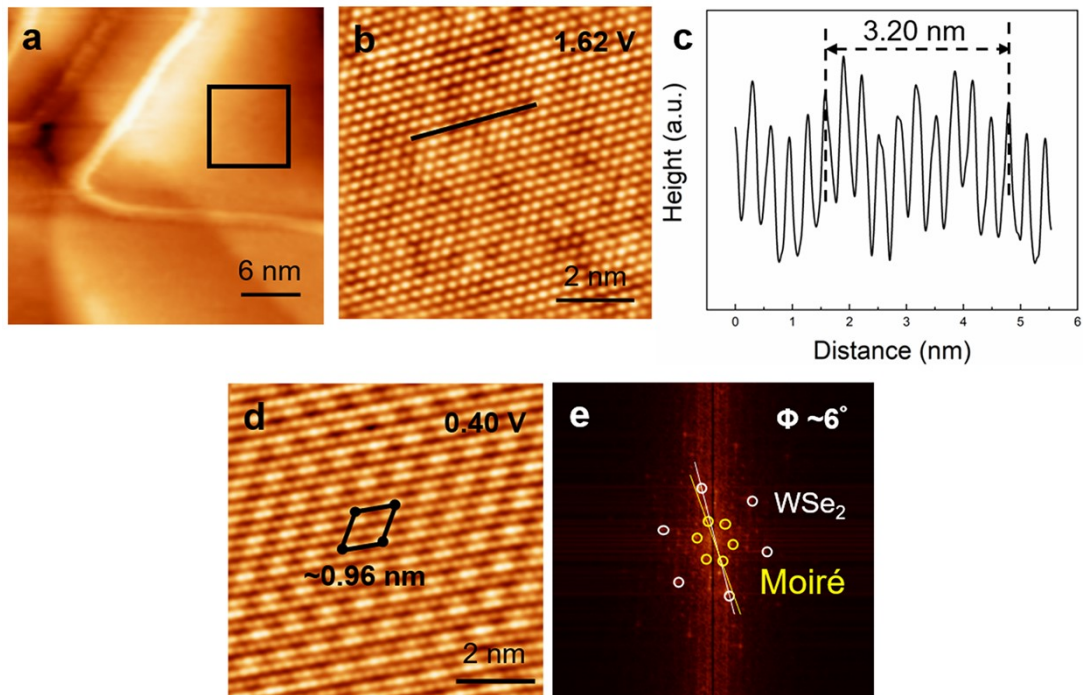


**Figure S4.** STM characterizations of monolayer  $\text{WSe}_2/\text{Gr}/\text{Au}$  vertical stack. (a) Large-scale STM image (1.63 V, 0.20 nA; 77 K) of monolayer  $\text{WSe}_2/\text{Gr}/\text{Au}$ . (b) Further magnification of the black rectangular region in (a). (c) Height profile along the black line in (b) showing a lattice constant of  $\sim 0.32$  nm indicating the formation of  $\text{WSe}_2$ . (d) STM topography of monolayer  $\text{WSe}_2/\text{Gr}/\text{Au}$  (as also shown in Figure 5c) in the main text. (e) The corresponding 2D fast Fourier transform (2D-FFT) pattern from (d). The orientation angle between the atomic row of monolayer  $\text{WSe}_2$  and the stripe direction of the moiré superstructure is  $\sim 6^\circ$ .

A large region of monolayer  $\text{WSe}_2/\text{Gr}/\text{Au}$  heterostructure is shown in Figure S4. Further magnification at the atomic scale image and its height profile shows a lattice constant of  $\sim 0.32$  nm, indicating the formation of monolayer  $\text{WSe}_2$ . The bias-dependent transition from the atomic lattice of monolayer  $\text{WSe}_2$  to the moiré pattern indicates the existence of monolayer  $\text{WSe}_2/\text{Gr}/\text{Au}$  heterostructure according to the structural simulation. The corresponding FFT image reveals the orientation angle between atomic row of monolayer  $\text{WSe}_2$  and the stripe direction of the moiré superstructure ( $\sim 6^\circ$ ).

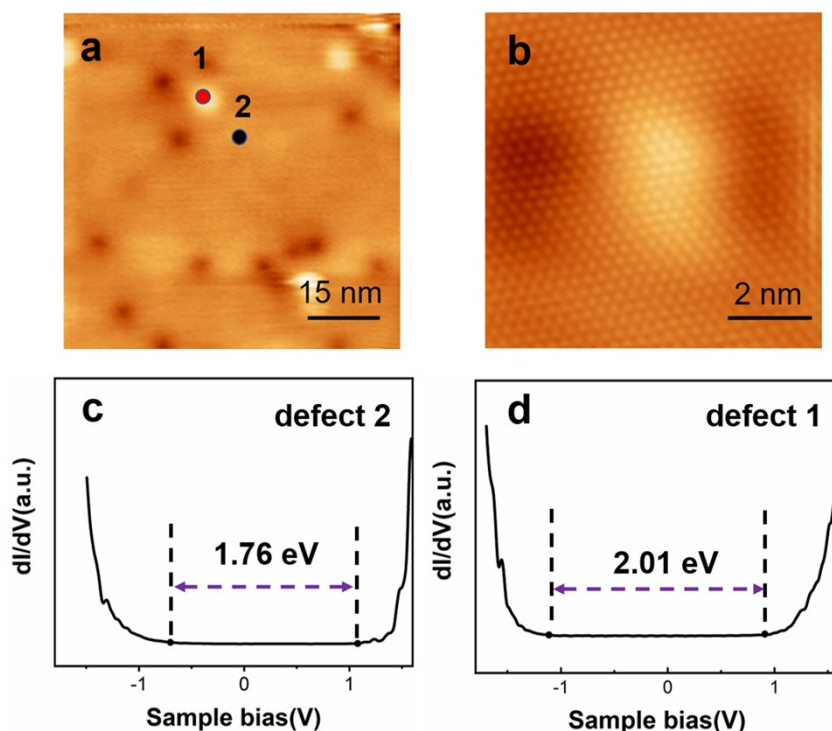


**Figure S5.** STM morphology of defect and defect-free areas for monolayer  $\text{WSe}_2/\text{Au}$ , and the corresponding STS spectra. (a) STM image (0.31 V, 0.20 nA; 77K) showing defect (bright protrusion marked by a red dot) and defect-free areas (marked by a black dot). The defects sites are characterized with dark spots or bright protrusions, corresponding to sulfur (S) vacancies or trapped atoms or molecules in the interfaces of monolayer  $\text{WSe}_2/\text{Au}$ . (b) Atomic resolution image (0.30 V, 0.20 nA; 77K) over the area in (a) marked with a red dot. (c-d)  $dI/dV$  spectra probed using STS at the defect-free areas (black dot) and the defect sites (red dot) from (a), respectively. (1.73 V, 0.80 nA, 10 mV, 932 Hz, 77K).

There are some light protrusions in the STM image, as shown in Figure S5 a. From successive zoom-in STM images in Figure S5 b, continuous crystal lattice can be observed to be decorated with dark or bright contrasts spots, corresponding to the sulfur (S) vacancies or trapped atoms or molecules in the interfaces of monolayer  $\text{WSe}_2/\text{Au}$ , respectively.

The STS spectra were collected with the STM tip positioned at the defect-free (black dot) and defect (red dot) regions, respectively. The VBM and CBM of the defect-free region are located at  $\sim -0.70$  eV and 1.06 eV, respectively, yielding a quasiparticle bandgap ( $E_g$ ) of  $\sim 1.76$  eV (Figure S5 c). At the defect site featured with bright protrusion (Figure S5 d), the VBM and CBM are located at  $\sim -1.11$  and 0.90 V, respectively, corresponding to band gap of  $\sim 2.01$  eV, very close to the intrinsic band gap of monolayer  $\text{WSe}_2$  on HOPG ( $\sim 2.12$  eV).<sup>1</sup> The interface trapped molecules or atoms are expected to weaken the interface coupling interaction between  $\text{WSe}_2$  and Au, leading to more intrinsic electronic band gap than that of  $\text{WSe}_2/\text{Au}$ .

## References

- 1 C. Zhang, Y. Chen, A. Johnson, M.-Y. Li, L.-J. Li, P. C. Mende, R. M. Feenstra and C.-K. Shih, *Nano Lett.*, 2015, **15**, 6494–6500.